Wear Behavior of Al6061/TiO₂ Composites Synthesized by Stir Casting Process

Ahmed Ali Gad El-Mawla, S. Z. El-Abden, Badran A. H.

Department of Production Engineering and Mechanical Design, Faculty of Engineering, Minia University, El-Minia 61111, Egypt
Corresponding Author email: ahmed.ali@minia.edu.eg

ABSTRACT

Aluminum, as a base metal in metal matrix composites (MMCs), has favor over other traditional materials in the scopes of aviation, space, automotive and marine applications because of their improved properties such as specific strength, good corrosion resistance. Wear behavior, as a major inferiority for Al6061, was tried to be improved by adding Titanium Dioxide (TiO₂) particles constituting a wear resistant composite that complies with tribological uses such as brakes. Composites reinforced with weight percentages 1:5 wt% of TiO₂ with step of 1% were prepared using stir casting technique. The addition of the TiO₂ deeply affected the wear performance of Al6061 alloy where the more the percentage of the reinforcement was added, the more the coefficient of friction was elevated where reinforced composite with 5 wt% of reinforcement particles showed highest coefficient of friction. In the other hand, the reinforced composite with 5 wt% TiO₂ had the biggest wear even, in some cases, more than the unreinforced alloy, while 2 wt% TiO₂-composite showed the lowest wear over friction process.

1. INTRODUCTION

The usage of aluminum based composite is escalating daily in the entire manufacturing areas due to their attractive properties such as high specific strength, good mechanical properties and better durability [1]. There is an immense demand for advanced engineering materials with high strength, light weight, and increased wear resistance in aviation, civil, and automobile applications specially sliding parts. This leads to the development of aluminum matrix composites (AMCs) [2, 3].

Al6061, as one of 6xxx alloys, is higher in corrosion resistance if compared with alloys from 2xxx & 7xxx series alloys. This advantage paves the road to its widespread use in marine and aerospace applications [4]. Other good characteristics of Al6061 are heat treatability and good formability which enable from its in structural applications [5]. the most inferiority

related to this alloy is its wear characteristics that have lower values in comparison with another aluminum series like 7xxx series and limited their use in certain tribological applications [6] .

So, researchers had directed their efforts to reach considerable developments on the level of the wear of Al6061 alloy by impeding hard phase such as ceramic particulates into Al6061 constituting a composite. Here strong nature of the hard phase delivers to the aluminum alloy with retaining its soft characteristics such as ductility.

Al6061 was reinforced with TiB₂ particles using stir casting process showing improvement in the wear resistance characteristics in terms of co-efficient of friction of the composite specimen with the increase in the amount of TiB₂ in the aluminum composite [7]. Also, the weight loss of the composite due to the wear test was detected that displayed increased loss in weight was

given with increase in the load applied in the pin-on-disc equipment.

Reinforcing Al6061 with Al_2O_3 was achieved using stir casting technique that introduced a composite with improved wear characteristics than the base alloy where pin-on-disc test showed considerable improvement in wear rate with increase of the reinforcement particles, also the amount of weight loss was decreased with the increase of Al_2O_3 content [8]. Optimization of pin-on-disc parameters using Taguchi's technique was applied to find the optimum conditions of dry sliding wear of Al 6061/rock dust composite synthesized by stir casting [9]. The applied load had been found having the highest statistical influence on the wear rate of the composite with a percentage contribution of (47.61%) more than all other factors such as reinforcement size, weight fraction of reinforcement sliding, velocity and sliding distance. Confirmation experiment was carried out and a comparison was made between experimental values and computed values, showing an error associated with dry sliding wear of composites varying from 3.10% to 6.59%.

Another attempt was achieved to improve wear behavior of Al6061 alloy by [10], this time by adding garnet particles using stir casting. Where a theoretical approach was developed beside the experimental work to detect the wear behavior whose results displayed improvement in wear resistance was related to the increasing of the reinforcement particles content.

There are different types available of ceramic particles used in MMCs, TiO_2 is one of them which is chemically inert [11], with superior corrosion resistance and high hardness and modulus [12]. Minerals as possible reinforcements have gradually arisen by counting the environmental considerations. Oxide phases widely get the fracture toughness of the materials better.

TiO_2 is available, has low cost and substantial resistance in wear, mechanical and thermal properties where [2] studied the wear behavior of hybrid composite reinforced with SiC & TiO_2 where results showed clear effect of TiO_2 on the level of wear where it displayed increase in coefficient of friction and decrease in weight loss with increasing TiO_2 for the same amount of SiC content. Another examination of TiO_2 addition on wear behavior of Al7068 composite was occurred by [13] who investigated the worn surfaces showing that the presence of TiO2 delivers extreme hardness to the composites reducing material loss.

Many methods are used to produce particulate metal matrix composite, stir casting is the most favorable one because of its cost effectiveness and simplicity leading to effective use in weight production [14, 15, 16]. Nano additives represent a frugal choice in mechanical and tribological applications [17, 18].

Aim of this work is to study the effect of pin-on-disc variables on Al6061-TiO_2 composite synthesized by stir casting in terms of the dry sliding wear behavior.

1. EXPERIEMENTAL WORK
1.1. Materials

Aluminum 6061 alloy was stir-cast with TiO_2 as reinforcement to fabricate Al6061/TiO_2 composites. The chemical composition of Al 6061 alloy is shown in Table 1. that provided from Helwan Company for Non-Ferrous Industries (Factory 63), Cairo, Egypt.

Table 1. Composition of Al6061 alloy (wt%)

Element	%
Al	97.5813
Si	0.71
Fe	0.11
Cu	0.22
Mn	0.0087
Mg	1.02
Zn	0.12
Cr	0.13
Ti	0.1

Some specifications of TiO_2 are introduced in Table 2. While Fig. 1. presents Scanning Electron Microscope images of as-received TiO_2 particulates showing their particle size using high resolution scanning electron microscope (model no. FEI Quanta FEG 250).

Table 2. TiO$_2$ specifications

Density (gm/cm^3)	3.97-4.05
Elastic modulus (GPa)	276-288
Hardness Vickers (GPa)	9.15-10.1
CTE (10^{-6}/°C)	8.4-11.8
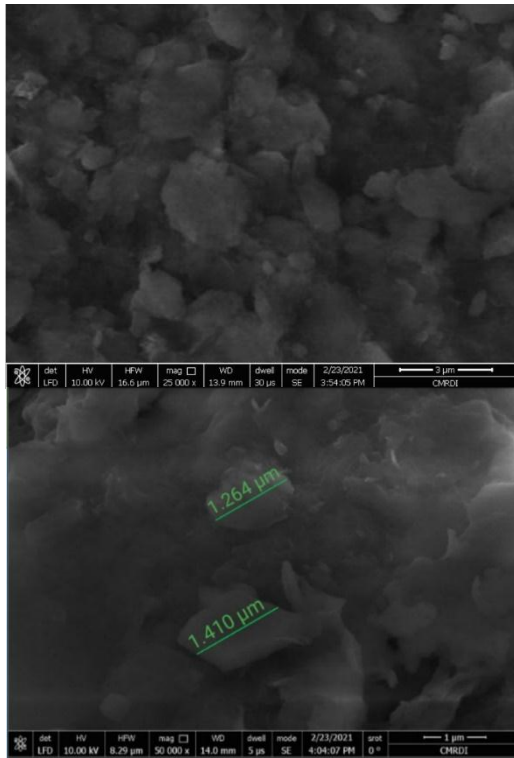
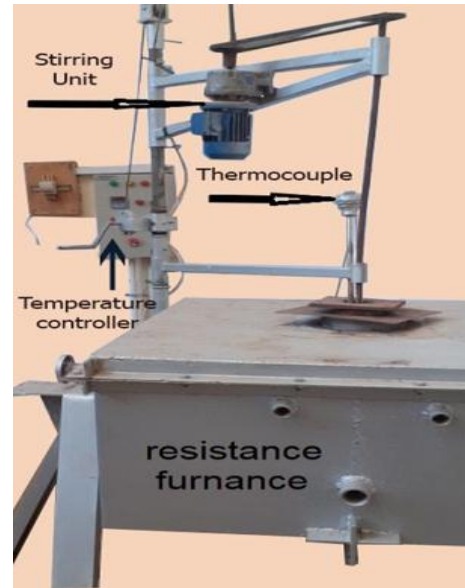Fig. 1. SEM micrographs of TiO$_2$

Fig. 2. Stir casting furnace

1.2. Microhardness and Wear test

The hardness of the reinforced samples had been measured using Vickers micro hardness tester (INNOVATEST NEMESIS 5101 Universal Hardness Tester) at room temperature state, on the polished surface. Each hardness value was the average of three randomly conducted indentations by applying load of 300 g for 15 s.

Pin-on-disc device was used to evaluate the coefficient of friction and the wear of the reinforced samples. The results were the average of 3 repeated tests for each specimen. The tests were conducted under dry laboratory conditions. The pin-on-disc setup is shown in Fig. 3.

Stir casting furnace, as shown in Fig. 2. was used to prepare reinforced Al6061 with TiO$_2$ where firstly, a pre-determined quantity of AA6061 alloy to be melt then a measured quantity of TiO$_2$ particles weighed using digital electronic weighing device was kept in a preheating furnace and preheated up to 500 °C. The preheated TiO$_2$ particles were added to the molten metal at 750 °C. The melt was subsequently stirred at 1000 rev/min for 10 min. using a stainless-steel stirrer. Then, the molten metal was poured into the preheated steel mold and the required composite was obtained. The same procedure was repeated for all other compositions. The cast Al 6061/TiO$_2$ composites were machined to the required specimen size for conducting various tests.
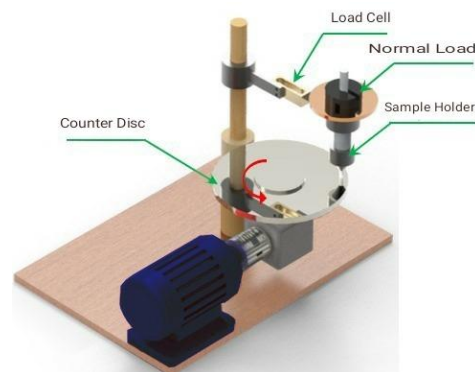

Fig. 3. Pin-On-Disc setup

Table 3. provides the applied values of the pin-on-disc parameters used in testing. The disc material is stainless steel with high smooth surface.

The composite samples were prepared as pins with regular dimensions of 8 mm in diameter & 20 mm in height. The. surface roughness of the test pin specimen and the disc were maintained at 80 μm. The weight loss of the pin was evaluated using an electronic weighing balance with an accuracy of 0.001 g.

Table 3. Values of pin-on-disc parameters

Parameter	Values
Applied loads (N)	6, 12 & 18
Sliding distance (m)	500, 1000, 1500, & 2000 [2]
Sliding velocity (m/s)	4.5, & 6.5

1.3. Microstructural examination

Worn surfaces had been observed through microstructural examinations. Microstructural study was analyzed with an Olympus BX51 light microscope. Images were recorded by a digital camera (Olympus DP 73) attached to the microscope using Cell Sense Imaging software (Olympus).
Reinforced samples were prepared for microscopic examination through Polishing process to obtain mirror-like surface then passing it through an etchant consisting of 0.5 ml HF in 100 ml water [19].

2. RESULTS AND DISCUSSIONS
2.1. Density and porosity

The density of the composites had been experimentally calculated by the Archimedean approach using small pieces cut from the composite samples [18, 19 & 20]. Additionally, the theoretical density was evaluated using the mixture rule based on the known densities of the matrix phase and TiO_2 particulates that are 2.7 and 4.05 g/cm^3, respectively.
The impact of the reinforcement percentage on the detected porosity of the composite samples is shown in Fig. 4. It resulted that the porosity amount percentage rises with increasing the

weight content of reinforcement particles [21, 22 & 23]. This is basically because of the effect of gas entrapped during stirring process [26].
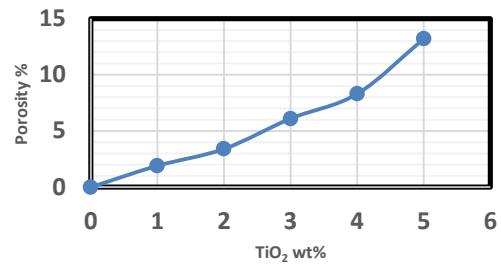

Fig. 4. The variation of porosity with TiO_2 particle content

2.2. Microhardness

microhardness values of Al6061 and the reinforced composites with weight percentages of TiO_2 is shown in Fig. 5. It was observed that the increase in reinforcement content increases the correspondent microhardness. The grain refinement and increased dislocations density due to the presence of reinforcing particles, alongside the basically hard nature of the TiO_2 particles are the direct reasons of improving the hardness outputs [27].
The increasing porosity, accompanied to the increase in reinforcing particles, presented negative effect of microhardness values where it helps produce more deep indentations during testing but the positive effects of the uniform presence of TiO_2 vanishes the porosity effect.
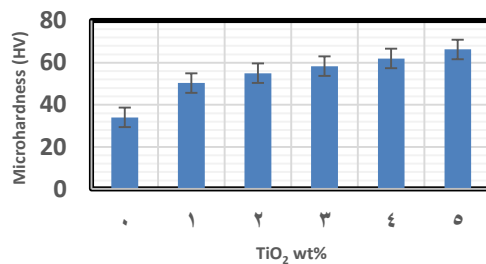

Fig. 5 microhardness values of Al6061 reinforced with TiO_2 particle percentage

2.3.   Investigation of microstructure

Microstructure of as cast Al6061 and reinforced Al6061 are shown in Fig. 6 (A-F). The microstructure in the base alloy has primary α-Al dendrites (red circles) and eutectic silicon (yellow circles) as islands surrounded by aluminum [8 & 23], that shown in Fig. 6 (A) of pure Al6061 without any addition.

Grain structure was displayed with the presence of TiO_2. Figure 6 (B & C) of composites reinforced with 1wt%, 2wt% respectively, where grain boundary clearly reveals in indication to uniform scatter of TiO_2 particles over the composite that leads to refining grains [24, 25].

 Minimum grain size was found with 2% addition. Some tiny porosities over the specimen were observed (pointed by yellow arrows).

More big and clear porosities (indicated by yellow arrows & circle) over the matrix are revealed in Fig. 6 (D) of composite reinforced with 3wt% TiO_2 [31]. Appearance of dendritic structures was observed (red arrow & circle).
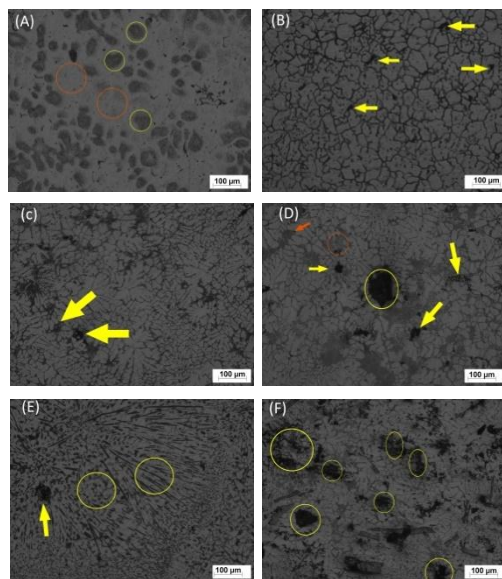

Fig. 6. The optical microphotographs of unreinforced and reinforced Al6061 alloy (A) 0%, (B) 1% (C) 2%, (D) 3%, (E) 4%, and (F) 5% TiO_2

Further, the micrographs expose smaller grain size of the reinforced composite more than the as-cast alloy with no particles where TiO_2

particles serve as heterogeneous sites for nucleation through solidification.

The tendency of clustering and agglomeration of TiO_2 has increased with increasing TiO_2 particulate content. This is clearly shown in Fig. 6 (E & F) of 4%, & 5% TiO_2, respectively, where clearly big porosities are shown (indicated by yellow arrows & circles). Further, increasing the fraction of reinforcement resulted in increase of porosity as pre-introduced in Fig. 4.

2.4.   Investigation of coefficient of friction

The impact of sliding distance and applied load on the coefficient of friction of unreinforced Al6061 alloy and reinforced composites with TiO_2 weight percentage for a sliding velocity of 4.5 m/s are outlined in Fig.7 (A-D). Where coefficient of friction versus sliding distance were introduced in Fig. 4 (A-C) with different applied loads 6, 12, & 18 N, respectively.

All graphs in Fig. 7. (A-C) showed increasing trend in coefficient of frictions with increase in reinforcement content. That is owing to elevated plastic strain grown when adhered reinforcing particles representing additional abrasives during sliding process, alongside with that the fraction of TiO_2 in the matrix increases, density of dislocation through the composites increases, which opposes plastic deformation developed from sliding process **[2].** Nonregular shape of the reinforcing particles, as shown in Fig. 1. produces additional resistance for sliding.

As shown in Fig. 7. (A), for sliding distance 500 m, it is observed that values of coefficients increase with increase in reinforcement percentage added to the composite. that observation was recorded for all conditions over graphs (A-C) in Fig. 7.

 for lower sliding distances, 500 & 1000 m, reinforced composites with 5 wt% TiO_2 presents the highest coefficient of friction for all applied loads. That is justified where the hard nature of reinforcement impeded through the matrix alloy delivers some reluctance to motion during the friction process leading to increase in coefficient of friction.

While, at longer sliding distances (1500 & 2000 m), some disparity is introduced where reinforced composite with 4 wt% TiO_2

occupies the most resistant composite in terms of coefficient of friction for applied loads 6 (Fig. 7. (A)) & 12 N (Fig. 7. (B)), while at loading with 18 N (Fig. 7. (C)), reinforced composite with 3 wt% TiO_2 presents the highest outcomes of coefficient of friction.

Graphs (A-C) of Fig. 7. Also showed that, for all alloy specimens – reinforced & unreinforced –with increase in sliding distance, there is a correspondent increase in coefficient of friction, where for an example, reinforced composite with 1% TiO_2 in Fig. 7. (A) presents increasing path of its values of coefficient of friction with increasing the sliding distance. That trend was repeated for all reinforced composites excepting reinforced alloys with 4%, & 5% TiO_2, that takes decreasing trend with increasing sliding distances, especially, at longer sliding distances such as 1500 & 2000 m.

Well distribution of reinforcement and low amount of porosity are the potential explanations for the reinforced composites with up to 3% of TiO_2 that they give increasing path of coefficient of friction values with increasing in sliding distances.

For reinforced alloys with 4%, & 5% TiO_2 that had a decreasing path of coefficient of friction values with increasing the sliding distances, that can be interpreted by the presence of porosity voids over the composite and agglomerated particles that contains voids.

Figure 7. (D) shows the variation of coefficient of friction respecting to the applied load for all reinforcement percentages and the unreinforced alloys at the maximum sliding distance (2000m). The coefficient of friction presents increasing path with increasing the applied load where highest coefficient of friction was recorded at loading with 18 N.
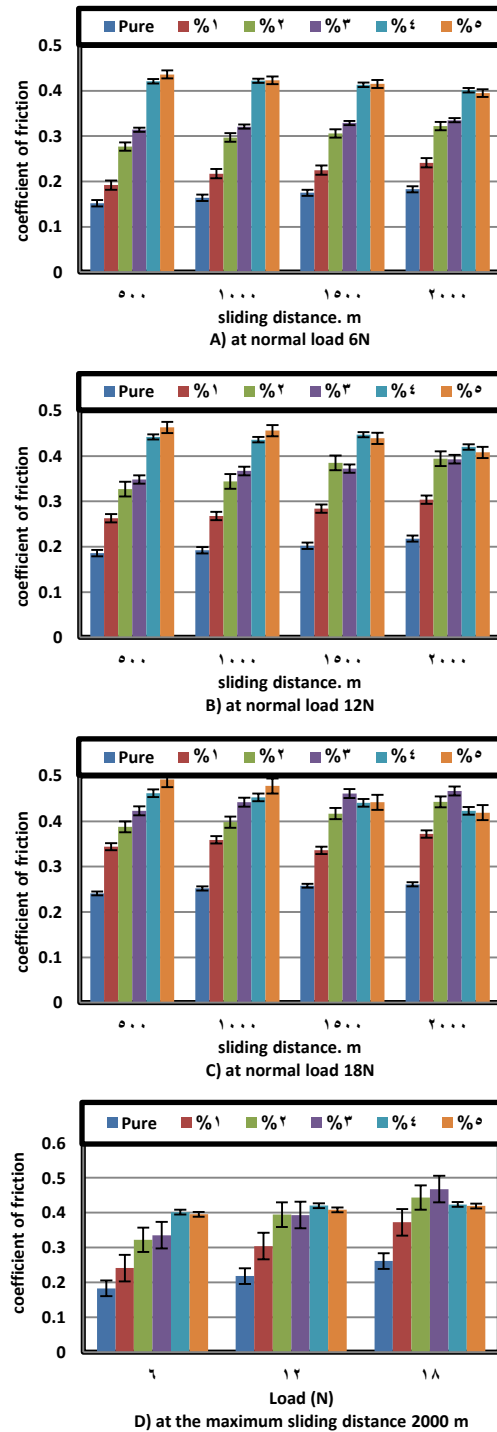

Fig. 7. Coefficient of friction over different sliding distances (A, B, & C) & different loads (D) at 4.5 m/s of unreinforced Al6061 & reinforced composites

Figure 8. (A-D) shows the effect of load and sliding distance on the coefficient of friction of unreinforced Al6061 alloy and reinforced composites with TiO_2 weight percentages but for a sliding velocity of 6.5 (m/s).

Similar trends as of sliding velocity 4.5 (m/s) of Fig. 7. are presented in Fig. 8. Of sliding velocity 6.5 (m/s) such as increasing path in coefficient of friction values with increasing the reinforcement percentages in the composites.

Where reinforced composite with 5 wt% of TiO_2, again, presents the highest coefficient of friction especially at lower sliding distances such as 500 & 1000 m for all values of applied loads (Fig. 8. (A-C)).

Reinforced composite with 4 wt% of TiO_2, in some cases at higher sliding distances (1500 & 2000 m) presents the highest coefficient at loading with 6 & 12 N, (Fig. 8. (A-B)). while Reinforced composite with 3 wt% of TiO_2 introduces the highest resistance to wear at the applied load 18 N, (Fig. 8. (C)).

Reinforced alloys with 4%, & 5% TiO_2, again adopt decreasing path in their outputted coefficient values with increasing sliding distances, especially, at longer sliding distances such as 1500 & 2000 m for all loading conditions (Fig. 8. (A-C)). As shown in Fig. 8. (A) where reinforced composite with 5% TiO_2 provides decreasing route of its values of coefficient of friction with increasing the sliding distance. That result was reiterated for all samples over graphs (A-C) in Fig. 8.

Another result was shown by Fig. 8. (A-D) when compared with Fig. 7. that with higher sliding velocity, values of coefficient of friction were shown bit to small higher values than with slower velocities. Where the levels of coefficient values at the higher sliding (6.5 m/s) velocities came higher than those obtained at the lower sliding speed (4.5 m/s). sliding velocity as a parameter of testing still marginally effects the wear outcomes in comparison with applied load or sliding distances.

Figures 7. (D) and 8. (D) again assert that the great effect of applied load on the coefficient of friction values where the increase in the load applied presents increase in the values of friction coefficient [33].
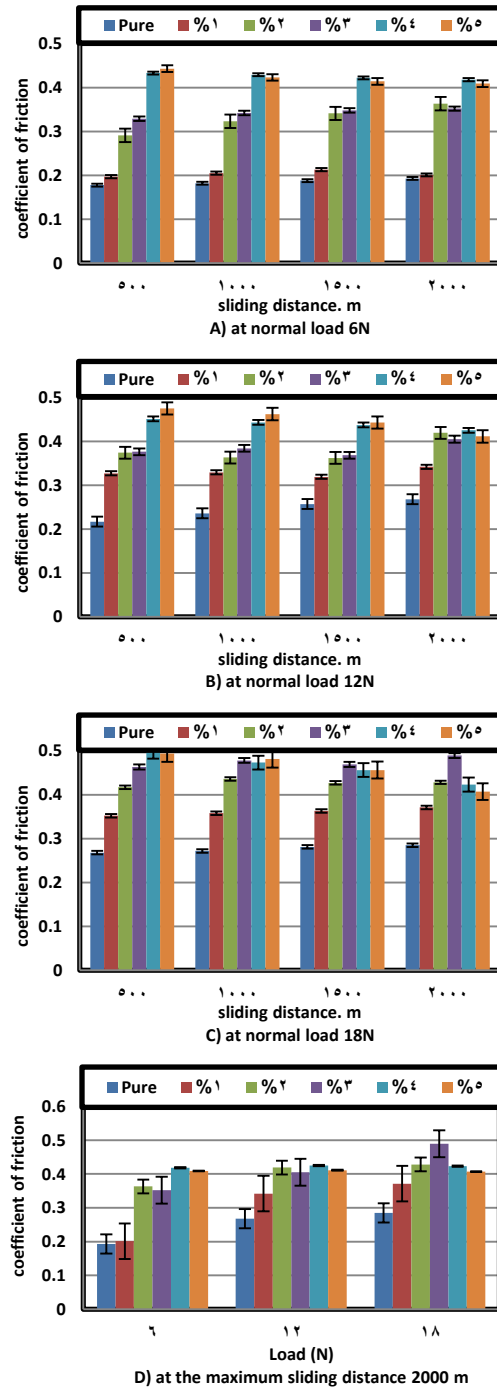

Fig. 8. Coefficient of friction over different sliding distances (A, B, & C) & different loads (D) at 6.5 m/s of unreinforced Al6061 & reinforced composites

2.5. Investigation of weight loss

The effect of load and sliding distance on the weight loss of unreinforced Al6061 alloy and reinforced composites with TiO_2 weight percentage for a sliding velocity of 4.5 (m/s) is plotted in Fig. 9. (A-D) Weight loss against sliding distance is introduced in Fig. 9. (A-C)

with various applied loads 6, 12, & 18 N, respectively.

Unreinforced composite presented higher loss in its weight over the friction process for all conditions of sliding distances and applied load, it may be clarified over the weak tribological nature of AA6061 which restricted its application for tribological uses [7].

Results showed that adding TiO_2 particles reduces weight loss of reinforced composites over fiction process, especially with weight percentages of reinforcement particles up to 2 wt% TiO_2, where higher percentages of reinforcement lead to increasing path of weight loss. Reinforced composites with 1 & 2 wt% of TiO_2 showed a clear enhancement in wear resistance of the AA6061, (Fig. 9. (A-C)) where values of weight loss dropped with the presence of reinforcement particles for all testing conditions. Reinforced composite with 2 wt% of TiO_2 had shown lowest recorded weight loss over the other composites. Uniformity of particle distribution and limited clustering of reinforcement particles, as shown in Fig. 6. (C), basically contributed to minimizing weight loss. As shown in Fig. 9. (B) with sliding distance 1000 m where weight loss takes decreasing route with adding TiO_2 till 2% then the value of the weight loss takes increasing path till 5% of reinforcement particles. That outcome was reiterated for all composites over graphs (A-C) in Fig. 9.

While reinforced composites with higher percentages, especially 4 & 5 wt%, presents higher loss in weight even than the unreinforced sample, in some cases, especially at longer sliding distances such as 1500 and 2000 m, that can be explained by the presence of agglomerated particles (Fig. 6. (E-F)) and porosity (Fig. 4.) that ease separation of material with friction.

All graphs show that weight loss increases with increase in sliding distance for all unreinforced and reinforced alloys where more distance means more time to friction that leads to more amount of loss in weight. That is observed at Fig. 9. (C) for reinforced composite with 2 wt% TiO_2 that presents increasing values of coefficient of friction with increasing in sliding distances of friction. That output was repeated for all samples over graphs (A-C) in Fig. 9.

Figure 9. (D) shows the variation of weight loss respecting to the applied load for all reinforcement percentages and the unreinforced alloys at the maximum sliding distance (2000m), where it was shown that increasing in applied load resulted in more wear rate [3, 32], asserting the large effect of load on the amount of weight loss.
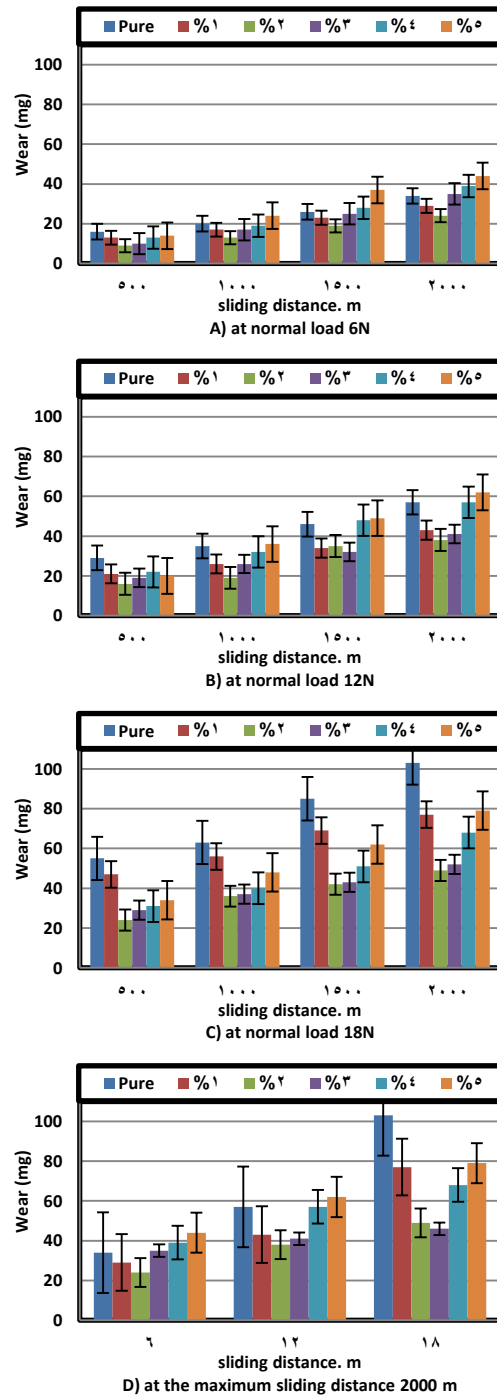

Fig. 9. Weight loss over different sliding distances (A, B, & C) & different loads (D) at 4.5 m/s of unreinforced Al6061 & reinforced composites

Figure 10. (A-D) shows the effect of sliding distance and load on the weight loss of unreinforced Al6061 alloy and reinforced composites with TiO$_2$ weight percentage for a sliding velocity of 6.5 (m/s).

some similar outcomes, like obtained in testing with 4.5 (m/s), were presented here with sliding speed 6.5 (m/s).

At the same conditions of sliding distance and the applied load in Fig. 10. It is always the pure alloy without reinforcement presents the highest amount of weight loss. But with some cases, Reinforced composite with 5 wt% of TiO$_2$, that have the largest amount of porosity, sometimes presented highest recorded value of weight loss especially at loading with 6 N as in Fig. 10. (A) and Fig. 10. (D).

The sliding speed affects the weight of the loss produced over the friction process where increase in sliding speed provides increase in weight loss amount. Sliding speed (6.5 m/s) gives clear effect on weight loss larger than that introduced by sliding speed (4.5 m/s), that is clear when comparing between outputs of figures 9 (A-D) & 10 (A-D), where the levels of weight losses obtained at the higher speed is higher than those of lower speed.

Increasing the applied load over the graphs of Fig. 10. (A-C) clearly contributes to increasing the resulted loss in weight.

Figure 10 (D) shows the variation of weight loss respecting to the applied load for all reinforcement percentages and the unreinforced alloys at the maximum sliding distance (2000m). The weight loss presents increasing route with increasing the applied load where maximum weight loss was recorded at load of 18 N.

Comparing between the figures 9. (D) and 10. (D) affirms that the value of the applied load has the vastest effect on weight loss values than sliding distance and sliding speed where the quantity of increase in weight loss with increase in of applied load is greater than with the increase of sliding distance.
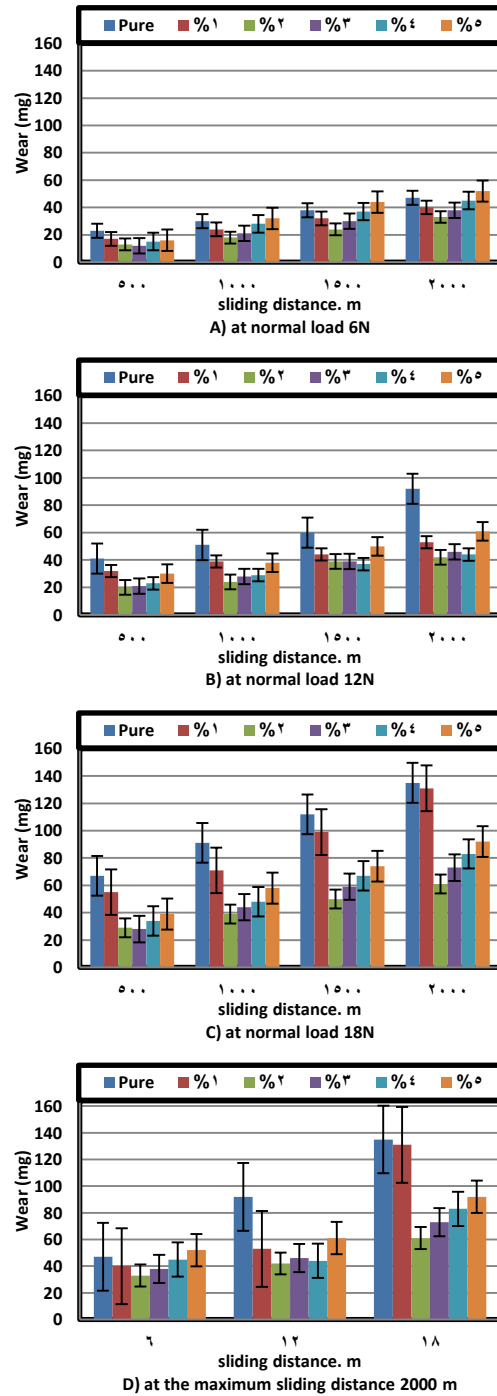

Fig. 10. Weight loss over different sliding distances (A, B, & C) & different loads (D) at 6.5 m/s of unreinforced Al6061 & reinforced composites

2.6. Investigation of worn surfaces

The worn surfaces of wear specimens are presented in Fig. 11. in two-dimensional and shadow three-dimensional views. Figure 11. (A) shows worn surface of unreinforced alloy that introduce clear apices (red points) spreading through the surface and some deep groves indicating low resistance to wear.

Figure 11. (B & C) of composites reinforced with 1% & 2% of TiO_2, respectively, introduce rather smooth worn surfaces with some minor cavities through the worn surfaces. The colored images of worn surfaces give lack of disparity in colors that means more resistant composite to wear. These smooth worn surfaces are because of the good distribution of the reinforcement over the matrix.

Figure 11. (D-F) of composites reinforced with 3%, 4%, & 5% of TiO_2, respectively, show some apices to appear again over the worn surfaces with larger cavities that can be explained upon the agglomeration of particles that leads to more porosities and easy separation of material during friction process.

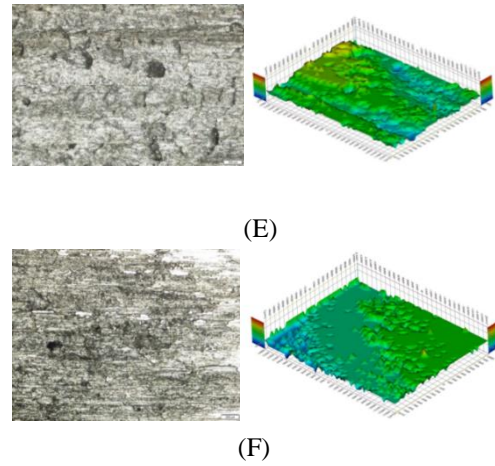

(A)

(B)

(C)

(D)

(E)

(F)

Fig. 11. Two-dimensional and Three-dimensional in shadow view images of a wear track of Al6061 alloy with (A) 0%, (B) 1% (C) 2%, (D) 3%, (E) 4%, and (F) 5% of TiO_2 at the testing conditions (18 N, 2000 m, & 6.5 m/s)

3. Conclusions

The dry sliding behavior of metal matrix composite (Al6061+TiO_2 particles) led to the following conclusions:

1. Optical micrographs exhibited uniform distribution of TiO_2 particles at 1 & 2 % wt% and clear clustering at 3, 4 & 5 wt% of reinforcement.

2. Porosity amount increases with increasing the reinforcement percentage.

3. The highest coefficient of friction was presented with 5 wt%-reinforced sample.

4. Reinforced composite with 2 wt% of reinforcement showed lowest Wear over friction test.
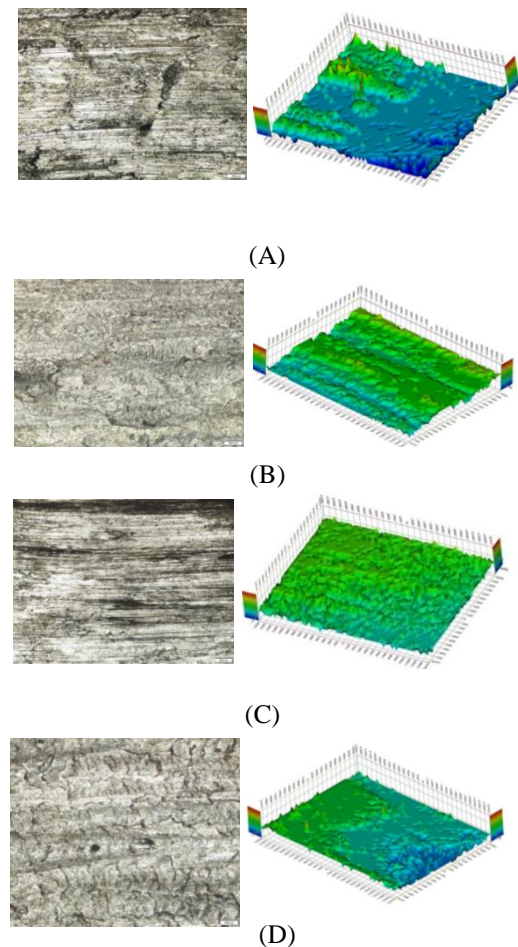
References

[1] A. Thirumoorthy, T. V. Arjunan, and K. L. Senthil Kumar, "Latest Research Development in Aluminum Matrix with Particulate Reinforcement Composites - A Review," *Mater. Today Proc.*, vol. 5, no. 1, pp. 1657–1665, 2018, doi: 10.1016/j.matpr.2017.11.260.

[2] C. A. V. Kumar and J. S. Rajadurai, "Influence of rutile (TiO2) content on wear and microhardness characteristics of aluminium-based hybrid composites synthesized by powder metallurgy," *Trans. Nonferrous Met. Soc. China (English Ed.*, vol. 26, no. 1, pp. 63–73, 2016, doi: 10.1016/S1003-6326(16)64089-X.

[3] G. Elango and B. K. Raghunath, "Tribological behavior of hybrid (LM25Al + SiC+ TiO2) metal matrix composites," *Procedia Eng.*, vol. 64, pp. 671–680, 2013, doi: 10.1016/j.proeng.2013.09.142.

[4] K. Ma, E. J. Lavernia, and J. M. Schoenung, "Particulate reinforced aluminum alloy matrix composites - A review on the effect of microconstituents," *Rev. Adv. Mater. Sci.*, vol. 48, no. 2, pp. 91–104, 2017.

[5] E. C. Moreno-Valle, I. Sabirov, M. T. Perez-Prado, M. Y. Murashkin, E. V. Bobruk, and R. Z. Valiev, "Effect of the grain refinement via severe plastic deformation on strength properties and deformation behavior of an Al6061 alloy at room and cryogenic temperatures," *Mater. Lett.*, vol. 65, no. 19–20, pp. 2917–2919, 2011, doi: 10.1016/j.matlet.2011.06.057.

[6] K. Umanath, K. Palanikumar, and S. T. Selvamani, "Analysis of dry sliding wear behaviour of Al6061/SiC/Al2O 3 hybrid metal matrix composites," *Compos. Part B Eng.*, vol. 53, pp. 159–168, 2013, doi: 10.1016/j.compositesb.2013.04.051.

[7] S. Suresh and N. S. V. Moorthi, "Process development in stir casting and investigation on microstructures and wear behavior of TiB2 on Al6061 MMC," *Procedia Eng.*, vol. 64, pp. 1183–1190, 2013, doi: 10.1016/j.proeng.2013.09.197.

[8] V. Bharath, M. Nagaral, V. Auradi, and S. A. Kori, "Preparation of 6061Al-Al 2 O 3 MMC's by Stir Casting and Evaluation of Mechanical and Wear Properties," *Procedia Mater. Sci.*, vol. 6, no. Icmpc, pp. 1658–1667, 2014, doi: 10.1016/j.mspro.2014.07.151.

[9] K. Soorya Prakash, A. Kanagaraj, and P. M. Gopal, "Dry sliding wear characterization of Al 6061/rock dust composite," 2015.

[10] S. C. Sharma, "The sliding wear behavior of A16061-garnet particulate composites," *Wear*, vol. 249, no. 12, pp. 1036–1045, 2001, doi: 10.1016/S0043-1648(01)00810-9.

[11] K. V. Shivananda Murthy, D. P. Girish, R. Keshavamurthy, T. Varol, and P. G. Koppad, "Mechanical and thermal properties of AA7075/TiO2/Fly ash hybrid composites obtained by hot forging," *Prog. Nat. Sci. Mater. Int.*, vol. 27, no. 4, pp. 474–481, 2017, doi: 10.1016/j.pnsc.2017.08.005.

[12] C. S. Ramesh, A. R. A. Khan, N. Ravikumar, and P. Savanprabhu, "Prediction of wear coefficient of Al6061-TiO2 composites," *Wear*, vol. 259, no. 1–6, pp. 602–608, 2005, doi: 10.1016/j.wear.2005.02.115.

[13] K. J. Joshua, S. J. Vijay, and D. P. Selvaraj, "Effect of nano TiO2 particles on microhardness and microstructural behavior of AA7068 metal matrix composites," *Ceram. Int.*, vol. 44, no. 17, pp. 20774–20781, 2018, doi: 10.1016/j.ceramint.2018.08.077.

[14] Yashpal, Sumankant, C. S. Jawalkar, A. S. Verma, and N. M. Suri, "Fabrication of Aluminium Metal Matrix Composites with Particulate Reinforcement: A Review," *Mater. Today Proc.*, vol. 4, no. 2, pp. 2927–2936, 2017, doi: 10.1016/j.matpr.2017.02.174.

[15] M. T. Sijo and K. R. Jayadevan, "Analysis of Stir Cast Aluminium Silicon Carbide Metal Matrix Composite: A Comprehensive Review," *Procedia Technol.*, vol. 24, pp. 379–385, 2016, doi: 10.1016/j.protcy.2016.05.052.

[16] D. R. J. Selvam and D. R. I. Dinaharan, "Synthesis and characterization of Al6061-Fly Ashp-SiCp composites by stir casting and compocasting methods," *Energy Procedia*, vol. 34, no. December, pp. 637–646, 2013, doi: 10.1016/j.egypro.2013.06.795.

[17] E. Ahmed, A. Nabhan, N. M. Ghazaly, and A. E. J. G. T, "Tribological Behavior of Adding Nano Oxides Materials to Lithium Grease : A Tribological Behavior of Adding Nano Oxides Materials to Lithium Grease : A Review," *Am. J. Nanometrials*, vol. 8,

no. January, pp. 1–9, 2020, doi: 10.12691/ajn-8-1-1.

[18] A. Nabhan and A. Rashed, "Effects of TiO 2 and SiO 2 Nano Additive to Engine Lubricant Oils on Tribological Properties at Different Temperatures," vol. 20, no. October, pp. 2463–2472, 2018.

[19] T. V. Christy, N. Murugan, and S. Kumar, "A Comparative Study on the Microstructures and Mechanical Properties of Al 6061 Alloy and the MMC Al 6061/TiB<sub>2</sub>/12<sub>p</sub>," *J. Miner. Mater. Charact. Eng.*, vol. 09, no. 01, pp. 57–65, 2010, doi: 10.4236/jmmce.2010.91005.

[20] H. R. Ezatpour, S. A. Sajjadi, M. H. Sabzevar, and Y. Huang, "Investigation of microstructure and mechanical properties of Al6061-nanocomposite fabricated by stir casting," *Mater. Des.*, vol. 55, pp. 921–928, 2014, doi: 10.1016/j.matdes.2013.10.060.

[21] H. R. Ezatpour, M. Torabi-Parizi, and S. A. Sajjadi, "Microstructure and mechanical properties of extruded Al/Al 2O3 composites fabricated by stir-casting process," *Trans. Nonferrous Met. Soc. China (English Ed.*, vol. 23, no. 5, pp. 1262–1268, 2013, doi: 10.1016/S1003-6326(13)62591-1.

[22] S. A. Sajjadi, H. R. Ezatpour, and M. Torabi Parizi, "Comparison of microstructure and mechanical properties of A356 aluminum alloy/Al2O3 composites fabricated by stir and compo-casting processes," *Mater. Des.*, vol. 34, pp. 106–111, 2012, doi: 10.1016/j.matdes.2011.07.037.

[23] M. Karbalaei Akbari, H. R. Baharvandi, and K. Shirvanimoghaddam, "Tensile and fracture behavior of nano/micro TiB2 particle reinforced casting A356 aluminum alloy composites," *Mater. Des.*, vol. 66, no. PA, pp. 150–161, 2015, doi: 10.1016/j.matdes.2014.10.048.

[24] J. Singh and A. Chauhan, "Characterization of hybrid aluminum matrix composites for advanced applications - A review," *J. Mater. Res. Technol.*, vol. 5, no. 2, pp. 159–169, 2016, doi: 10.1016/j.jmrt.2015.05.004.

[25] V. Ravi, C. R. P. Rao, and R. Suresh, "ScienceDirect Corrosion and Wear Studies On LM6 Grade Aluminum - Cenosphere Composite – An Experimental Approach," *Mater. Today Proc.*, vol. 5, no. 5, pp. 11667–11677, 2018, doi: 10.1016/j.matpr.2018.02.136.

[26] S. Chatterjee and A. B. Mallick, "Challenges in Manufacturing Aluminium Based Metal Matrix Nanocomposites via Stir Casting Route Challenges in manufacturing aluminium based metal matrix nanocomposites via stir casting route," no. January 2013, 2014, doi: 10.4028/www.scientific.net/MSF.736.72.

[27] W. S. Barakat, A. Wagih, O. A. Elkady, A. Abu-oqail, A. Fathy, and A. El-nikhaily, "Effect of Al 2 O 3 nanoparticles content and compaction temperature on properties of Al – Al 2 O 3 coated Cu nanocomposites," *Compos. Part B*, vol. 175, no. June, p. 107140, 2019, doi: 10.1016/j.compositesb.2019.107140.

[28] S. Sachinkumar, S. Narendranath, and D. Chakradhar, "Studies on microstructure and mechanical characteristics of as cast AA6061/SiC/fly ash hybrid AMCs produced by stir casting," *Mater. Today Proc.*, vol. 20, pp. A1–A5, 2020, doi: 10.1016/j.matpr.2020.01.266.

[29] B. Chandra Kandpal, J. Kumar, and H. Singh, "Manufacturing and technological challenges in Stir casting of metal matrix composites- A Review," *Mater. Today Proc.*, vol. 5, no. 1, pp. 5–10, 2018, doi: 10.1016/j.matpr.2017.11.046.

[30] D. P. Bhujanga and H. R. Manohara, "Processing and evaluation of mechanical properties and dry sliding wear behavior of AA6061-B4C composites," *Mater. Today Proc.*, vol. 5, no. 9, pp. 19773–19782, 2018, doi: 10.1016/j.matpr.2018.06.340.

[31] S. Gudipudi, S. Nagamuthu, K. S. Subbian, and S. P. R. Chilakalapalli, "Enhanced mechanical properties of AA6061-B4C composites developed by a novel ultra-sonic assisted stir casting," *Eng. Sci. Technol. an Int. J.*, no. xxxx, 2020, doi: 10.1016/j.jestch.2020.01.010.

[32] Y. Q. Wang and J. Il Song, "Dry sliding wear behavior of Al 2 O 3 fiber and SiC particle reinforced aluminium based MMCs fabricated by squeeze casting method," *Trans. Nonferrous Met. Soc. China (English Ed.*, vol. 21,

no. 7, pp. 1441–1448, 2011, doi: 10.1016/S1003-6326(11)60879-0.

[33] R. Harichandran and N. Selvakumar, "Microstructure and mechanical characterization of (B4C+ h-BN)/Al hybrid nanocomposites processed by ultrasound assisted casting," *Int. J. Mech. Sci.*, vol. 144, no. July 2017, pp. 814–826, 2018, doi:

10.1016/j.ijmecsci.2017.08.039.

[34] S. Gopalakrishnan and N. Murugan, "Production and wear characterisation of AA 6061 matrix titanium carbide particulate reinforced composite by enhanced stir casting method," *Compos. Part B Eng.*, vol. 43, no. 2, pp. 302–308, 2012, doi: 10.1016/j.compositesb.2011.08.049.